Title

Combinatorial optimization and spatial remodeling of CYPs to control product profile.

Authors

Yang, Jiazeng

Liu, Yuguang

Zhong, Dacai

et al.

Publication Date

2023-11-01

DOI

10.1016/j.ymben.2023.09.004

Peer reviewed

Metabolic Engineering 80 (2023) 119–129

Contents lists available at ScienceDirect

Metabolic Engineering

journal homepage: www.elsevier.com/locate/meteng

Combinatorial optimization and spatial remodeling of CYPs to control product profile

Jiazeng Yang [a,b,c], Yuguang Liu [b,c], Dacai Zhong [b,c], Linlin Xu [c], Haixin Gao [b,c], Jay D. Keasling [c,d,e,f,g], Xiaozhou Luo [a,b,c], Howard H. Chou [a,b,c,*]

[a] Shenzhen Key Laboratory for the Intelligent Microbial Manufacturing of Medicines, Shenzhen Institute of Advanced Technology, Chinese Academy of Sciences, Shenzhen, 518055, China
[b] CAS Key Laboratory of Quantitative Engineering Biology, Shenzhen Institute of Synthetic Biology, Shenzhen Institute of Advanced Technology, Chinese Academy of Sciences, Shenzhen, 518055, China
[c] Center for Synthetic Biochemistry, Shenzhen Institute of Synthetic Biology, Shenzhen Institute of Advanced Technology, Chinese Academy of Sciences, 518055, China
[d] Joint BioEnergy Institute, Emeryville, CA, 94608, USA
[e] Biological Systems and Engineering Division, Lawrence Berkeley National Laboratory, Berkeley, CA, 94720, USA
[f] Department of Chemical and Biomolecular Engineering & Department of Bioengineering, University of California, Berkeley, CA, 94720, USA
[g] Novo Nordisk Foundation Center for Biosustainability, Technical University of Denmark, 2800, Kgs. Lyngby, Denmark

A B S T R A C T

Activating inert substrates is a challenge in nature and synthetic chemistry, but essential for creating functionally active molecules. In this work, we used a combinatorial optimization approach to assemble cytochrome P450 monooxygenases (CYPs) and reductases (CPRs) to achieve a target product profile. By creating 110 CYP-CPR pairs and iteratively screening different pairing libraries, we demonstrated a framework for establishing a CYP network that catalyzes six oxidation reactions at three different positions of a chemical scaffold. Target product titer was improved by remodeling endoplasmic reticulum (ER) size and spatially controlling the CYPs' configuration on the ER. Out of 47 potential products that could be synthesized, 86% of the products synthesized by the optimized network was our target compound quillaic acid (QA), the aglycone backbone of many pharmaceutically important saponins, and fermentation achieved QA titer 2.23 g/L.

1. Introduction

Cytochrome P450 enzymes (CYPs) are a superfamily of versatile biocatalysts found throughout the biological kingdoms and known to catalyze more than 20 different types of oxidation reactions (Guengerich and Munro, 2013; Podust and Sherman, 2012). CYPs are best known for their ability to catalyze the regio- and stereo-selective oxidation of nonactivated C–H bonds in complex chemical scaffolds (Urlacher and Girhard, 2019). They play important roles in the biosynthesis of natural products such as terpenoids (Paddon et al., 2013), alkaloids (Zhang et al., 2022), and (iso)flavonoids (Sun et al., 2022). CYPs operate under mild conditions and can be more efficient than existing chemical catalysts (Li et al., 2020; Hammer et al., 2017), which makes them of interest to the pharmaceutical, chemical, and biotechnological industries.

The versatile role CYPs play in nature makes them an important tool in synthetic biology for building microbial cell factories (MCFs) to produce commercially valuable pharmaceuticals (Hu et al., 2023), such as saponins (Zhao and Li, 2018; Wang et al., 2020). Building MCFs to synthesize saponins is challenging, especially when the aglycone backbone needs to be oxidized at multiple carbon positions with differing degrees of oxidation necessary to enable the downstream acylation/-glycosylation reactions. All this must work in absolute synergy to achieve proper immunostimulant, antiviral, antifungal, antiparasitic, or antitumor activity (Güçlü-Ustündağ and Mazza, 2007; Reichert et al., 2019). *Quillaja saponaria* Molina (QsM) is the major source of saponins used in vaccines for the prevention of diseases (e.g., malaria, shingles, cancers, HIV-1, Covid-19) (Lacaille-Dubois, 2019; Laurens, 2020; Shah et al., 2019; Huang et al., 2020). The purification yield of the popular saponin QS-21 from QsM is ~0.001% (Walkowicz et al., 2016) and total chemical synthesis of QS-21 requires seventy-six steps (Fernández-Tejada et al., 2016), making both production methods economically challenging. Chemical synthesis of a QsM saponin can also begin with the triterpenoid quillaic acid (QA) (Wang et al., 2005), which is the aglycone backbone for 49 out of 58 saponins identified in QsM (Fleck et al., 2019). Recently, the *Q. saponaria* genome was sequenced and the genes expressing enzymes necessary for synthesis of QS-7 and the

* Corresponding author. Shenzhen Key Laboratory for the Intelligent Microbial Manufacturing of Medicines, Shenzhen Institute of Advanced Technology, Chinese Academy of Sciences, Shenzhen, 518055, China.
E-mail address: howard@siat.ac.cn (H.H. Chou).

https://doi.org/10.1016/j.ymben.2023.09.004
Received 1 August 2023; Received in revised form 7 September 2023; Accepted 8 September 2023
Available online 12 September 2023

bridgehead of QS-21 were elucidated and heterologously expressed in *Nicotiana benthamiana* (Reed et al., 2023).

Establishing a MCF to efficiently synthesize QA will provide a stable and scalable source of raw material for the synthesis of pharmaceutically important saponins. The biological pathway to synthesize QA requires multiple CYPs to oxidize β-amyrin (BA) at three different positions in a total of six oxidation steps: one-step oxidation at the C-16 position to a hydroxyl group, two-step oxidation at the C-23 position to an aldehyde group, and three-step oxidation at the C-28 position to a carboxyl group. It is known that CYPs can exhibit substrate promiscuity and oxidize unintended substrates (Bernhardt and Urlacher, 2014). The flexibility of CYPs in regard to substrate specificity can be useful for catalyzing new reactions, but can also lead to accumulation of under-oxidized or over-oxidized products not recognized by other co-expressed CYPs (Li et al., 2021; Moses et al., 2014). For example, each CYP could have multiple potential substrates and products during the conversion of BA to QA, leading to the synthesis of 47 different products (Fig. 1). Previously, BA was oxidized by two CYPs to produce QA, achieving a titer of 314 mg/L QA, specific productivity of 8–9 μg/L/h/OD_{600} QA, and QA made up only 54% of oxidized triterpenoids in a 5L fed-batch fermentation (Li et al., 2021). Low titer and purity increases purification costs due to the structural similarity between the side products and QA.

Recent efforts in synthetic biology to construct complex genetic circuits have used combinatorial optimization strategies to develop target phenotypes without prior knowledge about the expression levels of the component genes (Naseri and Koffas, 2020). Furthermore, most eukaryotic CYPs localize to the endoplasmic reticulum (ER) and function with a redox partner, cytochrome P450 reductase (CPR) (Nowrouzi and Rios-Solis, 2022). Different CPRs paired to the same CYP can affect the electron transfer efficiency between the CYP-CPR pair and can also lead to different product profiles (Sun et al., 2020). Therefore, we took a combinatorial optimization approach that constructed and iteratively screened CYP and CPR libraries without prior knowledge about the combination of enzymes that best performs any specific reaction. Rather than selecting for the most efficient CYP to catalyze each individual step, we iteratively screened different CYPs and CPRs in order to empirically build an enzyme network favoring QA production. By systematically constructing the enzyme network, the combinatorial optimization approach could potentially identify new CYP-CYP or CYP-CPR pairings that show improved activity, which might be missed using a targeted selection approach.

The spatial distance between CYPs could also affect final product distribution, because different CYPs prefer to localize on different ER membrane microdomains (Ozalp et al., 2005; Brignac-Huber et al., 2016). We hypothesized that manipulating the spatial configuration of the CYP network could lead to different product profiles. We discovered that expression of an *Arabidopsis thaliana* membrane steroid-binding protein (Gou et al., 2018) decreased the spatial distance between CYPs and significantly improved QA production. Finally, we overexpressed genes known to improve ER biogenesis (Kim, et al., 2019; Papagiannidis et al., 2021) in order to increase the ER surface available for binding by CYPs and CPRs and further improved QA production. Overall, a robust method that applies a combinatorial optimization strategy to build a heterologous CYP network and spatially controls the CYPs on the ER was developed. Implementation of this method achieved more than a 7-fold increase in titer, 32-fold increase in specific production, and QA consisted of 86% of oxidized triterpenoids.

2. Materials and method

2.1. Chemical compounds and standards

β-amyrin, hederagenin, echinocystic acid, and quillaic acid were purchased from Sigma-Aldrich (Shanghai, China), gypsogenin and gypsogenic acid were purchased from Toronto Research Chemicals (Toronto, Canada).

2.2. Genes and plasmids construction

The genomic DNA (gDNA) of *S. cerevisiae* CEN.PK2–1C was prepared using the DNAiso kit (Takara Biomedical Technology Co., Ltd., Beijing, China.) following the manufacturer's instructions. *Arabidopsis* complementary DNA (cDNA) was acquired following published protocol (Yang et al., 2020). Molecular cloning was accomplished using the Gibson Assembly® Cloning Kit (NEB). Native *S. cerevisiae* genes were amplified using *S. cerevisiae* CEN.PK2–1C gDNA as the template. *GgBAS*, *GvBAS*,

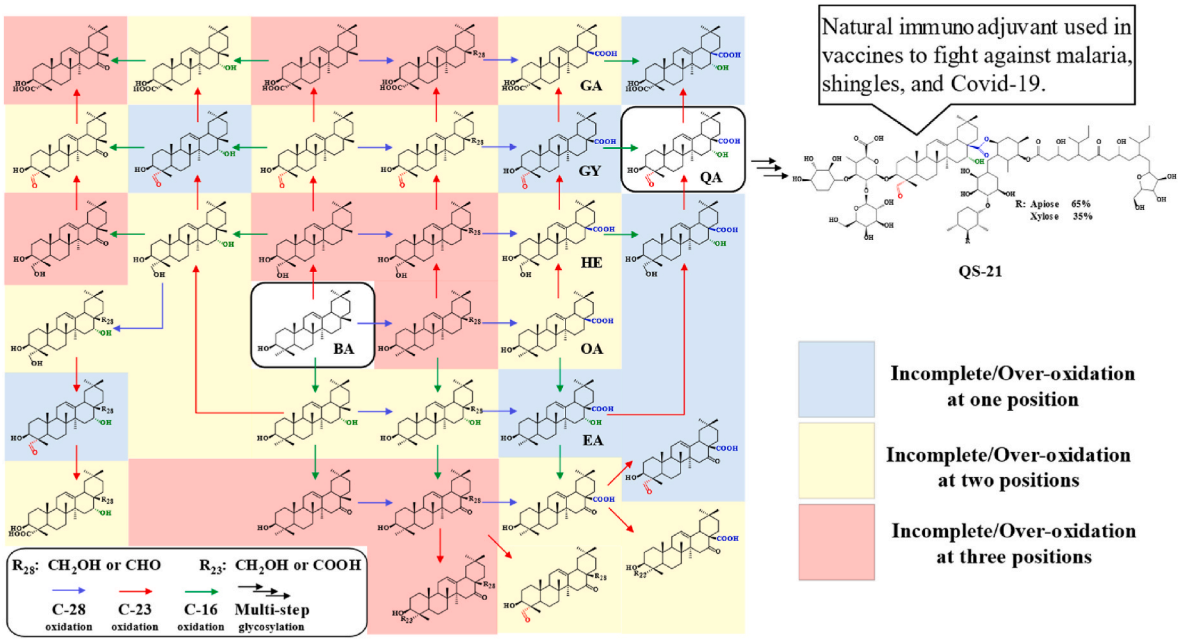

Fig. 1. Potential products formed from expressing CYPs to oxidize β-amyrin to quillaic acid. 47 different products can be formed during the six-step oxidation of β-amyrin at the C-16, C-23, and C-28 positions to produce quillaic acid. Quillaic acid is the biological precursor of the natural immunoadjuvant QS-21 and other *Quillaja saponaria* Molina saponins. BA: β-amyrin; OA: oleanolic acid; HE: hederagenin; GY: gypsogenin; EA: echinocystic acid; GA: gypsogenic acid; QA: quillaic acid.

and the CYP genes were codon-optimized, synthesized and cloned into pESC-URA plasmid by GENWIZ Inc (Suzhou, China). The *yfp* gene and the CPR genes were already available in the lab, with the exception of VvCPR, which was synthesized and codon-optimized by GENWIZ Inc. *AtBAS* and four MSBPs were amplified from *Arabidopsis* cDNA. All genes were expressed using native *S. cerevisiae* gal1/gal10 promoters or *Saccharomyces eubayanus* gal2 (SeGal2) promoter. The SeGal2 promoter was acquired according to published protocol (Peng et al., 2018). The combinatorial plasmid libraries were constructed using pESC-URA plasmid. The genotypes of the constructed plasmids, as well as the sequences of the genes and primers are listed in the Supplementary Tables 1, 2 and 4.

2.3. Strains construction

The strains used for combinatorial screening were constructed by transforming the combinatorial plasmid libraries in the target *S. cerevisiae* strains. Genomic integrations were performed using the Cas9-based method following published protocol (Luo et al., 2019). Cells were made competent using the Frozen-EZ Yeast Transformation II Kit (Zymo Research, CA, USA) according to the manufacturer's instructions. Transformed cells were plated on SD (synthetic defined) agar media supplemented with 2 g/L of glucose and lacking the appropriate nutrients for selection, and incubated at 30 °C for 4–5 days. Clones were screened using colony PCR and the gDNAs of positive clones were extracted, amplified, and sequenced for further validation. The constructed strains are listed in the Supplementary Table 3.

2.4. Flask cultivation

For plasmid expression experiments, three colonies of each engineered strain were separately inoculated into 10-mL test tubes containing 2 mL of SD media lacking the appropriate nutrients and supplemented with 2 g/L of glucose, incubated at 30 °C, and shaking at 220 rpm overnight. From each overnight culture, 1 mL starter culture was inoculated into a 250-mL flask containing 29 mL of SD media lacking the appropriate nutrients and supplemented with 2.0 g/L of galactose, grown at 30 °C, and shaking at 220 rpm for 96 h. For experiments where the heterologous genes are expressed from the chromosome, the protocol is similar to that of the plasmid expression experiments except that the fermentation used YPG media, which consists of 10 g/L of yeast extract, 20 g/L of peptone, and 20 g/L of galactose.

2.5. Fed-batch fermentation

The gDNA of yeast strain BY4742 was prepared by aforementioned method and used to clone the methionine and leucine auxotrophic maker genes. The two genes were integrated at the *rhr2* locus of strain yQA16G in order to create strain yQA20. Fed-batch fermentation was performed based on previous report (Yang et al., 2020) with a few adjustments. Single colonies of yQA20 were inoculated into 10-mL test tubes with 1 mL of YPD media, and the cultures were incubated overnight at 30 °C and 220 rpm. The overnight cultures were transferred into 250-mL flasks containing 29 mL of fresh YPG media and grown to OD_{600} 2–3. The resulting cultures were transferred to Eppendorf-DASGIP 1-L bioreactors (Eppendorf, Germany) containing 370 mL YPG media (pH 5.5), and pH was maintained by adding either ammonium hydroxide or 1 M HCl. Fermentations were performed at 30 °C, 400–800 rpm, and an air flow rate of 24 sL/h. Feed media A contained 400 g/L of galactose, which was fed at a rate of 1–4 mL/h to keep the DOC between 0% and 30%. Feed media B contained 50 g/L of yeast extract and 100 g/L of peptone, and was fed 24 h after inoculation at a rate of 1 mL/h for 40 h.

2.6. Western blotting

The western blot experiments were carried out according to previously published method with little modification. First, yeast expressing His-tagged CYPs or CPRs were inoculated into 10-mL test tubes containing 1 mL of SD media lacking uracil and supplemented with 2 g/L of glucose, incubated at 30 °C, and shaking at 220 rpm overnight. The cells were then transferred into 250-mL flask containing 29 mL of SD media lacking uracil and supplemented with 2.0 g/L of galactose, grown at 30 °C, and shaking at 220 rpm for 96 h 50 OD_{600} of cells were harvested by centrifugation, and the supernatant was discarded while the cells were resuspended in 5 mL of phosphate buffer solution (PBS) and lysed. After centrifuging at 13523 g, the supernatant was removed and the precipitate was re-dissolved using 1 mL 8 M urea. 10 μL of supernatant and dissolved precipitate were analyzed using 10% SDS-PAGE. The proteins were transferred onto a nitrocellulose membrane and detected with mouse monoclonal antiV5-fluo antibody (Proteintech, USA). Reading and analysis were carried out using a Tanon 5200 scanner (BioTanon, Shanghai, China). The CYPs and CPRs were only detected in the dissolved precipitate.

2.7. Triterpenoid extraction and analysis

Triterpenoid extraction and analysis were performed as previously described with minor adjustment (Li et al., 2020). Oleanolic acid, gypsogenin, gypsogenic acid, hederagenin, echinocystic acid, and quillaic acid were quantified using LC/MS. First, each culture was centrifuged at 2348 g to separate the supernatant from the cell pellet. The supernatant was discarded and acetone/methanol (1:1, v/v) was added to the cell pellet, and lysed using BeadBeater (BioSpec, USA) following the manufacturer's instructions. The lysed sample was centrifuged at 13523 g for 10 min, and 2 μl of sample was injected into an Agilent 1290 HPLC instrument equipped with an Agilent 6130 single-quadrupole MSD (Agilent Technologies, Santa Clara, CA, USA). Agilent ZORBAX Eclipse Plus C18 (3.5 μm, 2.1 × 100 mm) column (Agilent, USA) was used for chromatographic separation. The mobile phase consisted of acetonitrile (B) in 10% methanol solution with 0.1% acetic acid (A). The samples were run using the following condition: 0.00–20.00 min 50–59% B in A; 20.00–26.50 min 59–100% B in A; 26.50–29.00 min 100% B in A; 29.00–31.50 min 100-50% B in A; 31.50–34.00 min 50% B in A. β-amyrin was quantified using GC/MS. The samples were processed the same way as for LC/MS analysis except extraction was performed with n-hexane. After cell lysis, the samples were centrifuged at 13523 g for 10 min, and 200 μL of sample was placed in a new vial. N-hexane was evaporated using nitrogen gas and the residual solids were silylated with N-methyl-N-(trimethylsilyl) trifluoroacetamide (MSTFA) at 80 °C for 30 min and then dissolved in 1 mL of n-hexane prior to GC/MS analysis. GC/MS analysis was performed using an Agilent 8890B GC instrument equipped with an HP-5MS column and 5977B single quadrupole mass spectrometer in electron ionization (70 eV) mode. Generally, 1 μL of sample was injected at 80 °C, and held for 1 min before ramping the temperature at 20 °C/min to 300 °C and held for 15 min.

2.8. BiFC experiment

Bimolecular Fluorescence Complementation (BiFC) was performed using published protocol with minor changes (Ozalp et al., 2005). The yellow fluorescent protein (YFP) was split into two non-fluorescent fragments: nYFP (N-terminal 1–155 amino acid residues) and cYFP (C-terminal 156–242 amino acid residues). nYFP or cYFP was fused with a $(GSG)_4$ linker to CYP716A12, CYP716A262, and CYP72A567. The expression cassettes were inserted into either pESC-URA or pESC-LEU plasmids using the Gibson assembly method. Fluorescence experiments were performed using a Nikon AX microscope (Nikon, Japan) fitted with a × 60 oil-immersion objective. YFP was excited using a 488 nm laser and detected at 520–555 nm. Image analysis was carried out

using the NIS-Elements software.

2.9. Statistical analysis

All experiments were carried out with three independent replicates and data are expressed as mean ± standard deviation. Statistical analysis was performed using ANOVA in the Prism v.9 software (GraphPad Software). Statistical significance is indicated as *P < 0.1, **P < 0.01, ***P < 0.001, and ****P < 0.0001. No significance is presented as "ns".

3. Results

3.1. Construction of BA production chassis

We constructed a microbial chassis to produce the pentacyclic triterpenoid substrate BA that was used to screen CYPs for building an enzyme network to synthesize QA. First, three β-amyrin synthases (BAS) were screened by plasmid expression in *Saccharomyces cerevisiae* strain CenPK.2-1C: *A. thaliana* BAS (AtBAS) (Shibuya et al., 2009), *Glycyrrhiza glabra* BAS (GgBAS) (Zhang et al., 2015), and *Gypsophila vaccaria* BAS (GvBAS) (Meesapyodsuk et al., 2007), which produced 0.433 mg/L, 4.03 mg/L, and 4.02 mg/L BA, respectively. To increase carbon flux through the mevalonate (MVA) pathway and further increase BA titer, *Enterococcus faecalis* genes *mvaE* and *mvaS* were introduced at the *ura3-52* locus to improve mevalonate synthesis, and the native mevalonate pathway genes (*Erg12*, *Erg8*, *Erg19*, *IDI1*, *Erg20*, and *Erg9*) were overexpressed to improve farnesyl pyrophosphate (FPP) synthesis (Luo et al., 2019) (Supplementary Fig. 1a, Supplementary Table 3), creating strain JWY603. Expression of a plasmid encoding GvBAS in JWY603 improved BA production to 56.3 mg/L (Supplementary Fig. 1b). Integrating the gene encoding GvBAS into JWY603 at the *308a* locus created strain yQA05C, which produced 48.3 mg/L BA.

3.2. Establishment of a CYP network for QA production

Position C-28 in BA requires the highest number of oxidation steps, and thus has the highest probability of producing the largest number of potential output compounds. Therefore, initial enzyme networks were separately seeded with five CYPs hypothesized to solely oxidize BA at C-28 in order to understand the extent of oxidation at C-28. CYP716A12 from *Medicago truncatula* (Carelli et al., 2011), CYP716A75 from *Maesa lanceolata* (Moses et al., 2015), CYP716A83 from *Centella asiatica* (Kim et al., 2018), CYP716A94 from *Kalopanax septemlobus* (Han et al., 2018), and CYP716AL1 from *Catharanthus roseus* (Huang et al., 2012) were co-expressed on a plasmid with *A. thaliana* CPR 1 (ATR1), a commonly used CPR for screening plant CYP activity in heterologous hosts (Moses et al., 2014, 2015; Carelli et al., 2011; Kim et al., 2018; Han et al., 2018; Huang et al., 2012). The five CYP-ATR1 pairs were screened for production of the three-step oxidized product oleanolic acid (OA). Out of the CYPs co-expressed with ATR1, expression of CYP716A12 led to the most OA produced (14.5 mg/L) (Supplementary Fig. 2). The genes encoding CYP716A12 and ATR1 were integrated into yQA05C at the *911b* locus to create strain yQACYP1, which produced 22.7 mg/L OA.

Next, C-23 oxidation activity was added to yQACYP1, since this position contains the second largest number of oxidation steps. CYP714E19 from *C. asiatica* (Kim et al., 2018), CYP72A397 from *K. septemlobus* (Han et al., 2018), CYP72A68V2 from *M. truncatula* (Fukushima et al., 2013), and CYP72A567 from *Psammosilene tunicoides* (Li et al., 2021), were separately expressed from a plasmid and screened for the two-step oxidized product gypsogenin (GY). Screening these four CYPs mainly led to accumulation of either the under-oxidized product hederagenin (HE) or the over-oxidized product gypsogenic acid (GA). Although expression of CYP72A567 produced 2.33 mg/L GY, expansion of the network in yQACYP1 with C-23 oxidation activity did not accumulate the desired two-step oxidized product GY as the major product (Supplementary Fig. 3a).

Finally, the enzyme network in yQACYP1 was modified to include the one-step C-16 oxidation activity. CYP87D16 from *M. lanceolata* (Moses et al., 2015), CYP71Y16 from *Bupleurum falcatum* (Moses et al., 2014), and CYP716A262 from *P. tunicoides* (Li et al., 2021), were expressed from a plasmid and screened for the one-step oxidized product echinocystic acid (EA). Screening three CYPs showed that expression of CYP716A262 led to the highest EA titer at 7.74 mg/L. CYP716A262 was reported to oxidize BA to EA by catalyzing both C-16 and C-28 oxidations (Li et al., 2021). Integrating the genes encoding CYP716A262 and ATR1 on the chromosome of yQA05C to create strain yQACYP11 produced 3.87 mg/L EA, and expressing an additional copy of CYP716A262 from a plasmid in yQACYP11 produced 5.20 mg/L EA, which was 32.9% lower than EA produced by the network co-expressing the genes encoding CYP716A12 and CYP716A262 in yQACYP1 (Fig. 3a). The higher production in yQACYP1 compared to yQACYP11 suggested that the high EA titer observed using yQACYP1 was not due to the individual activity of CYP716A262, but a result of CYP716A12 and CYP716A262 functioning together.

The difference in EA produced by yQACYP1 and yQACYP11 suggests that different co-expressed CYPs and CPRs could affect the screening results. As a result, the four C-23 oxidizing CYPs were screened in yQACYP11 and compared to the screening results from yQACYP1. In yQACYP11, co-expression of CYP72A68V2 still led to GA being the major C-23 oxidized product, but co-expression of CYP714E19 and CYP72A567 led to QA being the major C-23 oxidized product (Supplementary Fig. 3b). In general, western blot analysis confirmed that the majority of the CYPs expressed well (Supplementary Fig. 10a), and protein level did not directly correlate with production level or resultant product profiles.

3.3. Effect of different CPRs on the CYP network

CPRs play an important role in modulating CYP activity by controlling electron transfer from nicotinamide adenine dinucleotide phosphate (NADPH) to CYP. We screened CPRs from different biological kingdoms (fungi, plant, animal) in order to determine how different CPRs affect CYP network activity, and whether plant CYPs in the network have preferences for plant CPRs. The 9 CPRs screened were: ATR1 and ATR2 from *A. thaliana* (Moses et al., 2014; Gou et al., 2018), CrCPR from *C. roseus* (Huang et al., 2012), AaCPR from *Artemisia annua* (Paddon et al., 2013), RoCPR from *Rosmarinus officinalis* (Yang et al., 2020), SaCPR from *Santalum album* (Diaz-Chavez et al., 2013), GlCPR from *Ganoderma lucidum* (Yang et al., 2018), GsCPR from *Ganoderma sinense* (Zhu et al., 2015), and AmCPR from *Apis mellifera* (Wallberg, et al., 2019).

CPRs were added to the networks separately seeded with CYPs oxidizing BA at C-28, creating 45 CYP-CPR pairs in yQA05C. Expression of each CPR created a unique activity profile, and expression of the ATR1 homolog ATR2 decreased OA by >63.9% compared to ATR1 (Supplementary Fig. 2), despite ATR1 and ATR2 expressing equally well (Supplementary Fig. 10b). Expression of either ATR1 or CrCPR led to stable OA production independent of the CYP expressed. Therefore, the genes encoding CYP716A12 and CrCPR were also integrated onto the chromosome of yQA05C at the *911b* locus to create strain yQA06A. By exchanging the CPR from ATR1 (yQACYP1) to CrCPR (yQA06A), OA production increased by 85.6%–206 mg/L in YPG medium (Supplementary Fig. 4).

Next, the CYPs that oxidize at C-16 and C-23 were screened again in yQA06A and compared to the screening results from yQACYP1 in order to determine how changing CPR affects the CYP network. In general, OA, EA and GY titers increased, while HE (under-oxidized) and GA (over-oxidized) titers decreased, with the exception that HE titers increased when CYP72A567 was expressed in yQA06A compared to yQACYP1 (Supplementary Fig. 3c). The C-16 and C-23 oxidizing CYPs were also separately co-expressed with each CPR to create 63 CYP-CPR pairs, and each pair was screened in yQA06A (Fig. 2). Although pairs

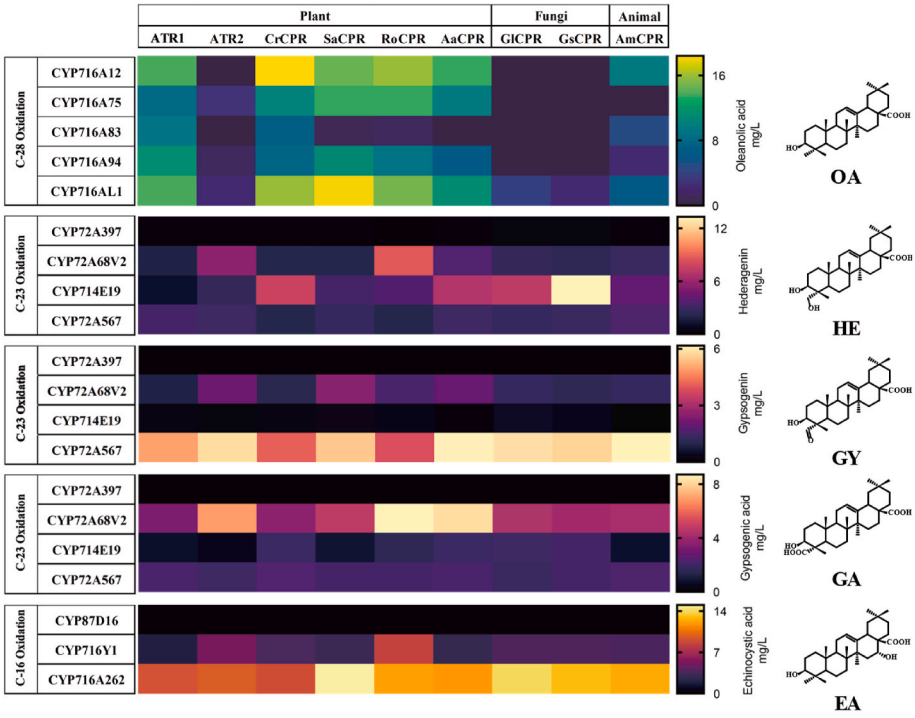

Fig. 2. Combinatorial optimization identifies novel CYP-CYP and CYP-CPR pairings for specific oxidase activities. C28 oxidation: combinatorial expression of 5 CYPs and 9 CPRs in strain yQA05C to evaluate oleanolic acid production. C-23 oxidation: combinatorial expression of 4 CYPs and 9 CPRs in strain yQA06A to evaluate hederagenin, gypsogenin, and gypsogenic acid production. C-16 oxidation: combinatorial expression of 3 CYPs and 9 CPRs in strain yQA06A to evaluate echinocystic acid production.

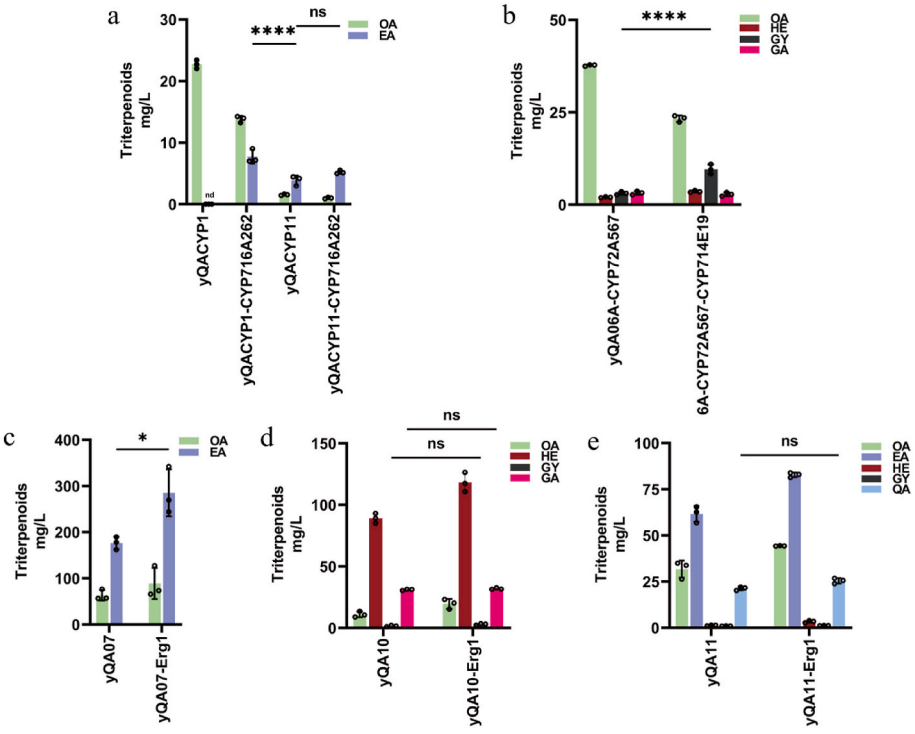

Fig. 3. CYP activities and product distribution are context dependent. a, Heterologous expression of CYP716A262 in a strain co-expressing CYP716A12 (yQACYP1) improves EA titer more than in a strain expressing a second copy of CYP716A262 (yQACYP11). **b**, Effect of co-expressing CYP714E19 and CYP72A567 to oxidize at the C-23 position and produce GY in strain yQA06A. n.d. (not detected).Perturbing the metabolic flux by overexpressing *erg1* improved EA titer in strain yQA07 (**c**), improved HE titer but not GA titer in strain yQA10 (**d**), and did not improve QA titer in strain yQA11 (**e**). The strain information is listed in Supplementary Table 3.

with ATR2 showed lower activity compared to pairs with ATR1 for C-28 oxidation, certain pairs with ATR2 showed higher activity compared to pairs with ATR1 for C-16 and C-23 oxidation. In some cases, pairs with ATR2 showed higher activity than pairs with CrCPR despite yQA06A already expressing a copy of CrCPR on the chromosome. Regardless of the paired CPR, CYP714E19 preferred to accumulate the C-23 single-oxidation product HE, CYP72A567 preferred to accumulate the C-23 double-oxidation product GY, and CYP72A68V2 preferred to accumulate the C-23 triple-oxidation product GA (Fig. 2, Supplementary Fig. 5). In general, CYPs that oxidize C-28 prefer plant CPRs. There was no clear preference for plant, fungal or animal CPRs observed for the CYPs that oxidize at C-16 and C-23, but higher activity was observed when CYP714E19, CYP72A567, and CYP716A262 was paired with certain fungal or animal CPRs compared to plant CPRs. These observations indicate that plant CYPs do not necessarily prefer plant CPRs in heterologous systems.

Vitis vinifera CPR (VvCPR) was previously paired with CYP716A262 and CYP72A567 to produce QA (Li et al., 2021). Expression of these two

CYP-CPR pairs in yQA06A did not increase activity compared to the other CYP-CPR pairs (Supplementary Fig. 5d and Supplementary Fig. 7). CYP716A262 paired with VvCPR only produced 1.31 mg/L EA, whereas paired with SaCPR led to 8.13 mg/L EA in yQA05C (Supplementary Fig. 7b). Not only did CPRs impact EA titer dramatically in yQA05C, CPRs also impacted product distribution as measured by the ratio of EA to OA (1.40:1 for VvCPR, 2.73:1 for ATR1, 3.02:1 for CrCPR, 2.58:1 for SaCPR, 1.13:1 for RoCPR, and 5.68:1 for AaCPR).

3.4. Understanding the impact of perturbing metabolic flux

Engineering metabolic flux towards increasing precursor supply is a common strategy to improve product titer and yield of MCFs (Paddon et al., 2013), and typically assumes reactions function in series, moving an accumulated substrate towards the next product in the pipeline. However, CYPs in the QA production network is assumed to function as a random network of reactions, so three different CYP networks were created to understand how metabolic flux perturbations impact a random network of reactions. The enzyme network in yQA06A was expanded with C-16 oxidation activity by integrating the gene encoding CYP716A262 to create the EA producing strain yQA07. To create enzyme networks with C-23 oxidation activity, the gene encoding CYP72A68V2 was integrated into yQA06A to create HE and GA producing strain yQA10, and the gene encoding CYP72A567 was integrated into yQA07 to create QA producing strain yQA11.

Perturbation of the CYP networks in yQA07, yQA10, and yQA11 was achieved by overexpressing *S. cerevisiae* squalene epoxidase *erg1* to increase 2,3-oxidosqualene production. Metabolic flux perturbation increased total triterpenoid titer by 30.1–55.8%, increased the relative amount of single-step oxidation products (EA and HE), but had no significant impact on the relative amount of multi-step oxidation products (GY, GA and QA) (Fig. 3c, d, e). If cofactors (e.g., NADPH) or CPR were limiting, then EA or HE would not have increased with increased precursor supply. Therefore, this data suggests that using the traditional technique of increasing precursor supply to increase target product production is more complicated in metabolic pathways containing multiple CYPs, especially when multi-step oxidation reactions are involved.

3.5. Expansion of the CYP network to improve QA production

To determine which oxidation reactions might be limiting, the network in yQA11 was expanded by rescreening the 12 CYPs oxidizing C-28, C-23, and C-16 and inserting them at the *met15* locus. Addition of five CYPs that oxidize at C-28 improved QA production by up to 29.4%, addition of the four CYPs that oxidize at C-23 improved QA production by 68.9–110%, and addition of the three CYPs that oxidize at C-16 improved QA production by 46.8–78.1% (Fig. 4a). Out of the 12 CYPs screened, adding one additional copy of the gene encoding CYP72A567 (strain yQA12J) increased QA titer the most, with QA titer reaching 44.7 mg/L, but adding two additional copies of CYP72A567 (strain yQA12N) did not further improve QA titer despite EA titer decreasing significantly (Supplementary Fig. 8a). However, co-expression of the genes encoding CYP714E19 and CYP72A567 (strain yQA12P) improved QA production by 49.7%–64.7 mg/L compared to yQA12N. The genes encoding CYP714E19 and CYP72A567 were also co-expressed in yQA06A to create strain yQA06-C8C9 to determine whether the improvement in C-23 oxidation is dependent on the other CYPs in the network. Co-expression of the two CYPs in yQA06A improved GY production by 210% (Fig. 3b), indicating that the improvement in C-23 oxidation activity was not dependent on the other CYPs overexpressed in yQA11.

CPRs were shown to impact enzyme network activity, and 10 CPRs were rescreened by integrating them at the *ndt80* locus in yQA12P to determine how they impact QA production. Adding an additional copy of CrCPR (strain yQA13C) did not significantly improve QA titer, but adding SaCPR (strain yQA13F) to the network improved QA titer by 48.1% (Fig. 4b). According to the product distribution data from different CYP-CPR pairs (Fig. 2, Supplementary Figs. 5–7), addition of SaCPR to the network likely improved CYP72A567 and CYP716A262 activity, despite expression of SaCPR being relatively weak compared to the other CPRs (Supplementary Fig. 10b). Overall, optimizing the network for QA production by expanding the network in yQA11 with a copy of CYP714E19, SaCPR, and an additional copy of CYP72A567 increased QA production by 350% to 95.9 mg/L.

3.6. Spatial control of CYP network configuration

Reducing the spatial distance between enzymes of a biosynthetic pathway can improve production by MCFs (Park et al., 2022). CYPs can localize to different ER membrane microdomains. Therefore, extended physical distances between CYPs might lead to substrate or intermediate diffusion, resulting in either changes in product profile or reduced yield of the target compound. Membrane-associated progesterone receptors

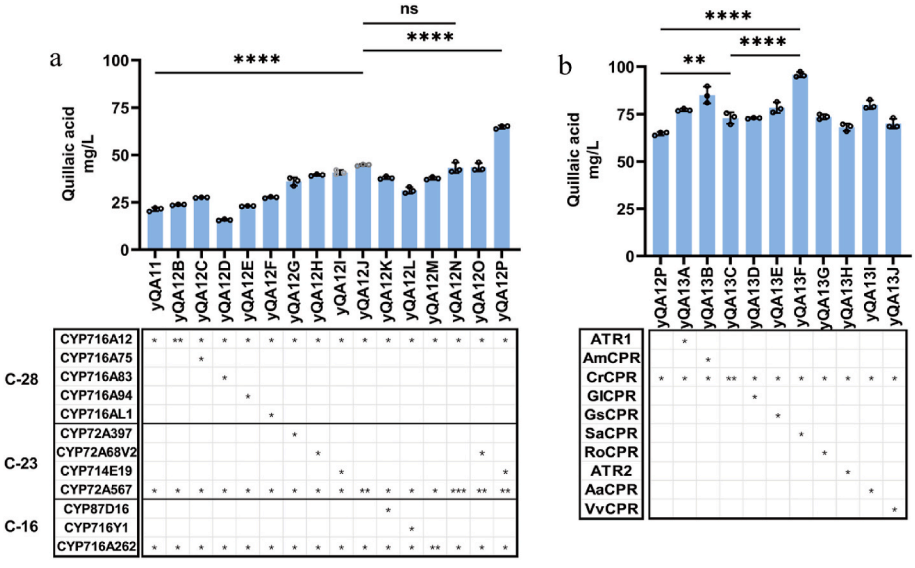

Fig. 4. Combinatorial expansion of enzyme network and taking advantage of network effects increased quillaic acid production. a, Quillaic acid titer of new strains established by rescreening the CYP library in strain yQA11, and **b**, rescreening the CPR library in strain yQA12P.

(MAPRs) are evolutionarily conserved proteins homologous to cytochrome *b*5 and can interact with CYPs to modulate their function (Ryu et al., 2017). MAPR orthologs, membrane steroid-binding protein 1 and 2 (MSBP1 and MSBP2), were discovered in *Arabidopsis* and regulate lignin biosynthesis by physically organizing CYPs on the ER membrane (Gou et al., 2018).

We attempted to use MSBPs to reorganize the physical network of heterologous CYPs on the ER, and hypothesized MSBPs could reduce the intermolecular distance between different CYPs during QA synthesis (Fig. 5a). The genes encoding *A. thaliana* MSBP1 and MSBP2, as well as two additional homologues MSBP3 and MSBP4 (Salanoubat et al., 2000; Mayer et al., 1999), were integrated into yQA11. QA titer improved by 71.2–91.7% when MSBP2-4 were expressed and improved by 223% when MSBP1 was expressed (Fig. 5b). Adding MSBP1 to the network in yQA11 improved the titer more than that observed after adding CYP714E19 and CYP72A567 to the network, indicating that proper physical network configuration is just as important for improving titer as the presence or absence of the component enzymes. The amount of other terpenoids did not change significantly after adding MSBPs, unlike when adding CYPs to the network, suggesting that MSBPs use a unique mechanism to improve QA titer (Supplementary Fig. 7). Adding MSBP1 to the network in yQA13F to create strain yQA15 led to an 79.5% increase in QA titer to 172 mg/L (Fig. 5c).

Bimolecular fluorescence complementation (BiFC) (Ozalp et al., 2005) was used to verify whether adding MSBP1 to the network actually reduced the intermolecular distances between CYPs. The gene encoding MSBP1 was integrated into JWY603 to create yQAM1. CYP716A12, CYP716A262, and CYP72A567 were fused with non-fluorescent fragments of yellow fluorescent protein (YFP), so that YFP signal can only be detected after different CYPs come in proximity to each other. No YFP signal was observed in JWY603 for CYP716A12-CYP716A262 and CYP716A12-CYP72A567 pairs, but YFP signal was observed for the same pairs when MSBP1 was present (Fig. 5d). These results indicate that MSBP1 changed the physical configuration of these enzymes in the cell. A faint YFP signal was observed for the CYP716A262-CYP72A567 pair in JWY603, and a stronger YFP signal was observed for the same

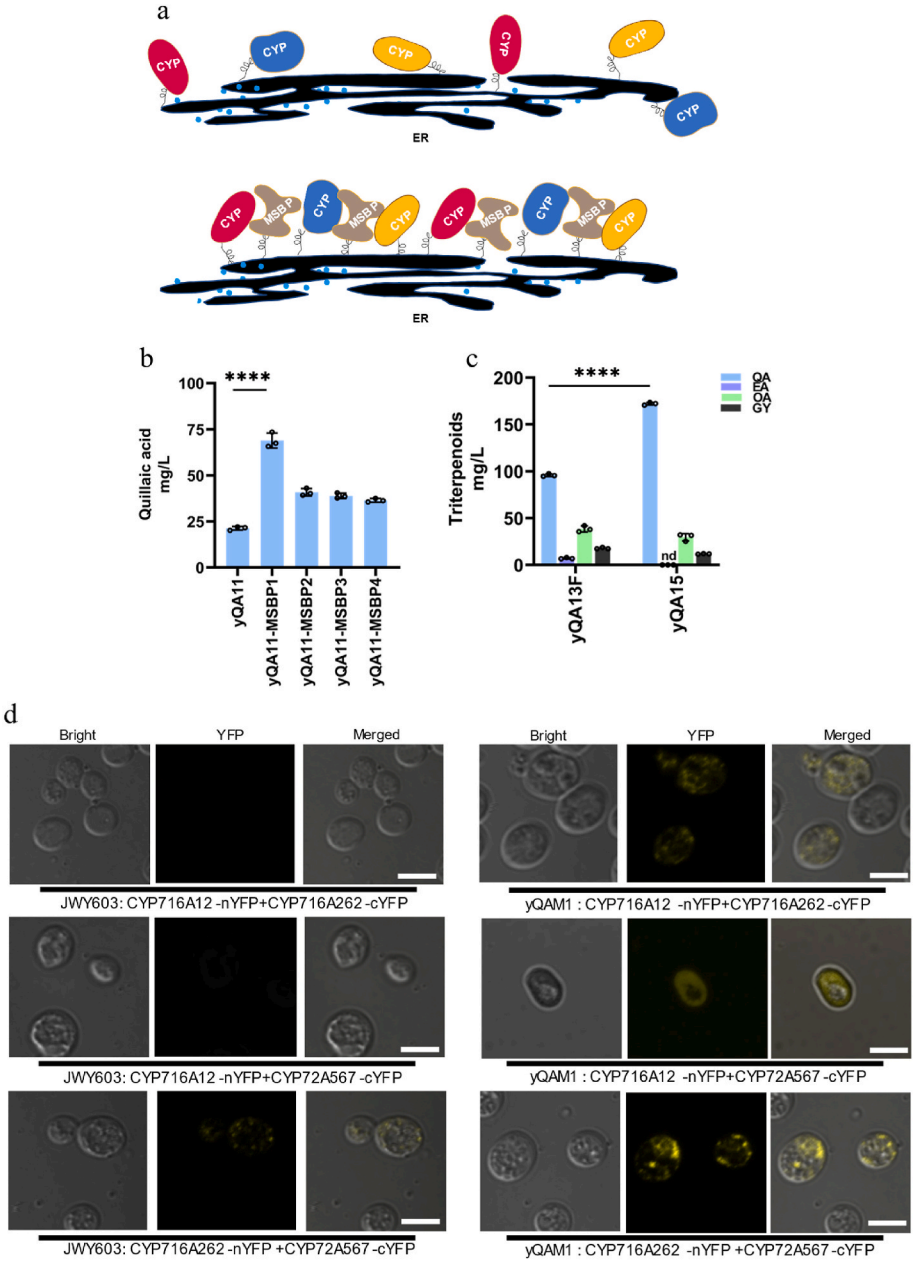

Fig. 5. Physical reconfiguration of spatial distance between CYPs on ER improved product profile. a, Model of protein complex formed between heterologous CYPs with and without MSBP present. **b**, Quillaic acid production after integrating four different MSBPs from *A. thaliana* into strain yQA11. **c**, Change in product profile and increase in quillaic acid production after adding MSBP1 to the enzyme network in yQA13F to create strain yQA15. n.d. (not detected). **d**, BiFC analysis of CYP716A12/CYP716A262 fused with nYFP, and CYP716A262/CYP72A567 fused with cYFP. Confocal images of strains JWY603 or yQAM1 (JWY603 expressing MSBP1) expressing different CYP pairs fused with either nYFP or cYFP. cYFP: C-terminal amino acid residues 156–242; nYFP: N-terminal amino acid residues 1–155. Bar = 5 μm.

pair in the presence of MSBP1, suggesting that the physical distance between CYP716A262 and CYP72A567 was further reduced in the presence of MSBP1. BiFC also confirmed that the three CYPs did not interact with themselves even in the presence of MSBP1 (Supplementary Fig. 11).

3.7. Sensitivity towards availability of NADPH and ER surface

CPRs transfer electrons from NADPH to CYP, so it is possible that NADPH regeneration is a limiting factor during QA production. Five enzymes catalyzing different mechanisms for NADPH regeneration (Partipilo et al., 2021; Li et al., 2018; Bieganowski et al., 2006) were added to the enzyme network in yQA11: *Escherichia coli* transhydrogenase SthA, *S. cerevisiae* NAD kinases Pos5 and Yef1, and *S. cerevisiae* dehydrogenases Ald6 and Tyr1. Out of the five enzymes screened, addition of SthA improved QA titer significantly by 186% (Supplementary Fig. 12). Furthermore, eukaryotic CYPs and CPRs must localize to the ER membrane in order to function. Previously, remodeling the ER by overexpressing *S. cerevisiae ino2* and *ice2* to increase ER size was shown to improve terpenoid production (Emmerstorfer et al., 2015). The large number of heterologous CYPs and CPRs in the enzyme network to synthesize QA suggests the availability of the ER surface could also be a limiting factor, so *ino2* and *ice2* were overexpressed in yQA11. Overexpression of *ino2* and *ice2* increased QA production by 60.4% and 152%, respectively (Supplementary Fig. 12). Finally, *sthA* and *ice2* were integrated individually and in combination into yQA15,

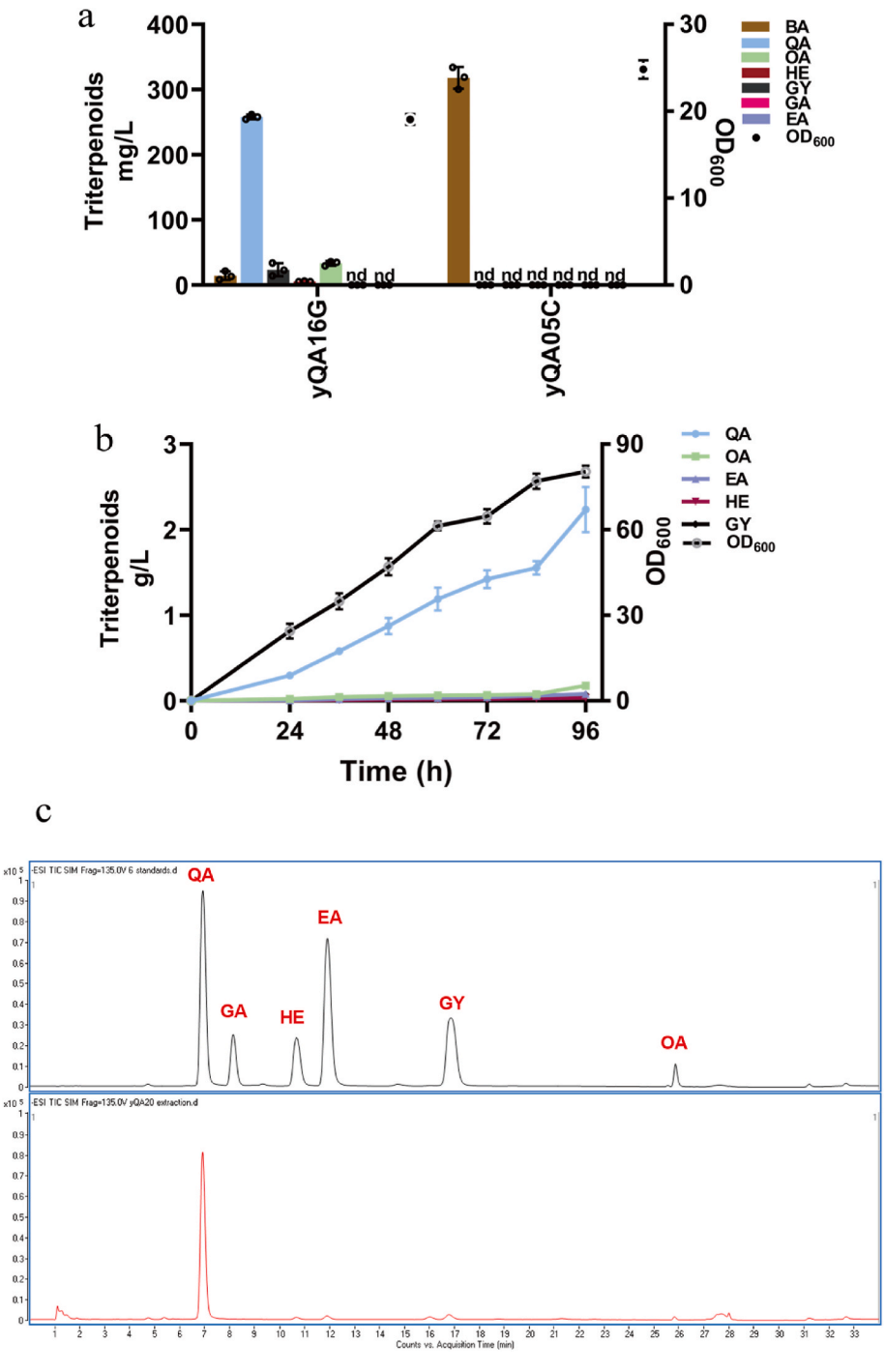

Fig. 6. Product profile of optimized CYP network primarily favors QA production. a, Triterpenoid titers produced by the starting strain yQA05C that only produces β-amyrin and final quillaic acid producing strain yQA16G that heterologously expresses the optimized CYP network. n.d. (not detected). **b**, Fed-batch fermentation of strain yQA20 to produce quillaic acid. **c**, LC-MS analysis results of quillaic acid, oleanolic acid, echinocystic acid, hederagenin, gypsogenin, and gypsogenic acid produced by yQA20 using negative ion mode in comparison with commercial standards.

and overexpression of both genes (strain yQA16G) improved QA titer the most to 258 mg/L (Supplementary Fig. 13).

Comparing the BA production strain yQA05C with the final QA production strain yQA16G (enzyme network consisting of CYP716A12, CYP714E19, two CYP72A567, CYP716A262, CrCPR, SaCPR, MSBP1; co-expressing SthA and Ice2) showed that the molar conversion of BA to QA was 71.2%, QA made up 80.6% of terpenoids, and QA titer achieved 258 mg/L in 250 mL flask fermentation (Fig. 6a). Finally, the leucine and methionine auxotrophies were removed in yQA16G to create strain yQA20. Fed-batch fermentation of yQA20 in 1L fermenters achieved a titer of 2.23 g/L QA, specific productivity of 290 μg/L/h/OD_{600} QA, and 86% of oxidized triterpenoids produced was QA (Fig. 6b and c).

4. Discussion

Our results demonstrate the feasibility of using a combinatorial optimization strategy to assemble an enzyme network that catalyzes the multi-step oxidation of inert substrates to synthesize functional scaffolds for building pharmaceutically active molecules. Using the combinatorial optimization strategy, we assembled an enzyme network to catalyze six oxidation steps at three different positions of β-amyrin to produce quillaic acid as the major product. By iteratively screening CYP and CPR libraries, two important observations were made.

Firstly, expressing a combination of different CYPs to catalyze multi-step oxidations at a particular carbon position can lead to higher production than increasing the copy number of the same CYP. Previously, it was shown that CYP716A262 can produce EA and its expression with CYP72A567 can produce QA (Li et al., 2021). The traditional strategy to enhance product titer would be to increase the copy number of these two enzymes. We showed that increasing CYP716A262 from one to two copies had limited effect on increasing EA titer, and increasing CYP72A567 from two to three copies had no effect on increasing QA titer. However, iteratively screening CYPs to build an optimal enzyme network led to the discovery that combining one copy of CYP716A12 with one copy of CYP716A262 was the best strategy for improving EA production. Similarly, the combination of two copies of CYP72A567 with one copy of CYP714E19 improved QA titer the most.

Secondly, CYP screening results can be dependent on the presence of other CYPs and CPRs, so care should be taken in the future when designing screens and interpreting results. Screening the same CYP-CPR library in the BA producing strain yQA05C and in the OA producing strain yQA06A produced different product distributions for each CYP-CPR pair. One might conclude that CYP716A262 has no preference for CPRs based on the screening results from yQA06A, but CYP716A262 showed a strong preference for SaCPR in yQA05C. The positive impact of adding SaCPR to the network was later confirmed in the QA producing strain yQA12P.

Metabolic engineering efforts typically increase flux towards precursor synthesis in order to push flux towards the target product and increase production titer. However, we observed that CYP networks are delicately balanced, especially when multiple oxidation steps are involved. Simply increasing precursor production can disrupt the product profile and lead to the accumulation of unwanted side products. Previous efforts to produce QA faced similar challenges and accumulated significant amounts of partially oxidized intermediates (Li et al., 2021). Rather than directly perturbing metabolic flux, we chose to manipulate the distance between different CYPs to increase target product synthesis. We showed that assembling the enzymes in the network into a proper spatial configuration is just as important as identifying which enzymes to add into the network towards increasing product titer and controlling product profile. We anticipate that these approaches will be generalizable and provide new strategies for assembling CYP networks for the synthesis of other pharmaceutically active molecules where multi-step oxidations are required. Enhancement of product distribution towards highly oxidized products, such as QA, might be further optimized by incorporation of additional enzymes that interact with CYP, such as cytochrome *b*5 (Kandel and Lampe, 2014).

While increasing gene expression (e.g., increasing promoter strength or gene copy number) is a common strategy in metabolic engineering, the iterative screening approach showed that multi-step oxidations by CYPs can be more efficient when catalyzed by limited expression of different enzymes rather than high expression of the same enzyme. This observation suggests that organisms in nature contain large libraries of CYPs, not only to target a diverse substrate pool, but also to take advantage of potential network effects that increase the catalytic efficiency for any particular reaction by having multiple different CYPs present. This hypothesis is further supported by our observation that bringing different CYPs in closer proximity to each other leads to increased activity towards the desired target profile. Finally, we provide a new framework for building CYP networks that is useful for discovering new reactions catalyzed by CYPs and constructing new biosynthetic networks catalyzed by multiple CYPs for synthesizing medicines and chemicals, and this framework enabled us to achieve the highest reported QA titer and productivity to date.

Synthesis of QS-21 requires functionalizing QA with eight sugars and one acyl group, which in theory could be performed in a microbial host by expressing genes identified from *Q. saponaria*. However, functional expression of an enzyme in a microbe does not necessarily lead to high enzyme activity, due to differences between the physicochemical microenvironments within microbial and plant cells, and the absence of helper proteins normally present in plant cells, as we showed in this work with MSBP. From a commercial perspective, low enzyme activity could be counterbalanced by the microbe's shorter production time and ease of scaling production relative to a plant-based system. Therefore, both microbial-based and plant-based production systems have unique advantages and challenges that need to be addressed in order to become stable sources of raw material for the production of adjuvants for vaccines.

Author contributions

J.Y. and H.H.C. conceived the project and designed the experiments. J.Y., Y.L., D.Z., H.G and L.X. performed the experiments. J.Y., X.L. and H.H.C. analyzed the results. J.Y., J.D.K and H.H.C. wrote and edited the manuscript.

Declaration of competing interest

X.L. has a financial interest in Demetrix and Synceres. J.D.K. has a financial interest in Amyris, Lygos, Demetrix, Maple Bio, Napigen, Apertor Pharma, Ansa Biotechnologies, Berkeley Yeast, and Zero Acre Farms. The other authors declare no competing interests.

Data availability

No data was used for the research described in the article.

Acknowledgements

We thank S.M. Ma and P.V. Chang for valuable advice editing the manuscript. This study was supported by grants from the National Key R&D Program of China (2020YFA0907700), Natural Science Foundation of China (22050410274 and 32101183), Bill & Melinda Gates Foundation (INV-025841), Guangdong Basic and Applied Basic Research Foundation (2021B1515020049 and 2023A1515011338), and China Postdoctoral Science Foundation (2020M682988).

Appendix A. Supplementary data

Supplementary data to this article can be found online at https://doi.org/10.1016/j.ymben.2023.09.004.

References

Bernhardt, R., Urlacher, V.B., 2014. Cytochromes P450 as promising catalysts for biotechnological application: chances and limitations. Appl. Microbiol. Biotechnol. 98, 6185–6203. https://doi.org/10.1007/s00253-014-5767-7.

Bieganowski, P., Seidle, H.F., Wojcik, M., Brenner, C., 2006. Synthetic lethal and biochemical analyses of NAD and NADH kinases in *Saccharomyces cerevisiae* establish separation of cellular functions. J. Biol. Chem. 281, 22439–22445. https://doi.org/10.1074/jbc.M513919200.

Brignac-Huber, L.M., Park, J.W., Reed, J.R., Backes, W.L., 2016. Cytochrome p450 organization and function are modulated by endoplasmic reticulum phospholipid heterogeneity. Drug Metab. Dispos. 44, 1859–1866. https://doi.org/10.1124/dmd.115.068981.

Carelli, M., Biazzi, E., Panara, F., Tava, A., Scaramelli, L., Porceddu, A., Graham, N., Odoardi, M., Piano, E., Arcioni, S., May, S., Scotti, C., Calderini, O., 2011. *Medicago truncatula* CYP716A12 is a multifunctional oxidase involved in the biosynthesis of hemolytic saponins. Plant Cell 23, 3070–3081. https://doi.org/10.1105/tpc.111.087312.

Diaz-Chavez, M.L., Moniodis, J., Madilao, L.L., Jancsik, S., Keeling, C.I., Barbour, E.L., Ghisalberti, E.L., Plummer, J.A., Jones, C.G., 2013. Bohlmann, J. Biosynthesis of sandalwood oil: *Santalum album* CYP76F cytochromes P450 produce santalols and bergamotol. PLoS One 8, e75053. https://doi.org/10.1371/journal.pone.0075053.

Emmerstorfer, A., Wimmer-Teubenbacher, M., Wriessnegger, T., Leitner, E., Müller, M., Kaluzna, I., Schürmann, M., Mink, D., Zellnig, G., Schwab, H., Pichler, H., 2015. Over-expression of ICE2 stabilizes cytochrome P450 reductase in *Saccharomyces cerevisiae* and *Pichia pastoris*. Biotechnol. J. 10, 623–635. https://doi.org/10.1002/biot.201400780.

Fernández-Tejada, A., Tan, D.S., Gin, D.Y., 2016. Development of improved vaccine adjuvants based on the saponin natural product QS-21 through chemical synthesis. Acc. Chem. Res. 49, 1741–1756. https://doi.org/10.1021/acs.accounts.6b00242.

Fleck, J.D., Betti, A.H., Da Silva, F.P., Troian, E.A., Olivaro, C., Ferreira, F., Verza, S.G., 2019. Saponins from *Quillaja saponaria* and *Quillaja brasiliensis*: particular chemical characteristics and biological activities. Molecules 24, 171. https://doi.org/10.3390/molecules24010171.

Fukushima, E.O., Seki, H., Sawai, S., Suzuki, M., Ohyama, K., Saito, K., Muranaka, T., 2013. Combinatorial biosynthesis of legume natural and rare triterpenoids in engineered yeast. Plant Cell Physiol. 54, 740–749. https://doi.org/10.1093/pcp/pct015.

Gou, M., Ran, X., Martin, D.W., Liu, C.J., 2018. The scaffold proteins of lignin biosynthetic cytochrome P450 enzymes. Nat. Plants 4, 299–310. https://doi.org/10.1038/s41477-018-0142-9.

Guengerich, F.P., Munro, A.W., 2013. Unusual cytochrome p450 enzymes and reactions. J. Biol. Chem. 288, 17065–17073. https://doi.org/10.1074/jbc.R113.462275.

Güçlü-Ustündağ, O., Mazza, G., 2007. Saponins: properties, applications and processing. Crit. Rev. Food Sci. Nutr. 47, 231–258. https://doi.org/10.1080/10408390600698197.

Hammer, S.C., Kubik, G., Watkins, E., Huang, S., Minges, H., Arnold, F.H., 2017. Anti-Markovnikov alkene oxidation by metal-oxo-mediated enzyme catalysis. Science 358, 215–218. https://doi.org/10.1126/science.aao1482.

Han, J.Y., Chun, J.H., Oh, S.A., Park, S.B., Hwang, H.S., Lee, H., Choi, Y.E., 2018. Transcriptomic analysis of *Kalopanax septemlobus* and characterization of KsBAS, CYP716A94 and CYP72A397 genes involved in hederagenin saponin biosynthesis. Plant Cell Physiol. 59, 319–330. https://doi.org/10.1093/pcp/pcx188.

Huang, L., Li, J., Ye, H., Li, C., Wang, H., Liu, B., Zhang, Y., 2012. Molecular characterization of the pentacyclic triterpenoid biosynthetic pathway in *Catharanthus roseus*. Planta 236, 1571–1581. https://doi.org/10.1007/s00425-012-1712-0.

Huang, W.C., Zhou, S., He, X., Chiem, K., Mabrouk, M.T., Nissly, R.H., Bird, I.M., Strauss, M., Sambhara, S., Ortega, J., Wohlfert, E.A., Martinez-Sobrido, L., Kuchipudi, S.V., Davidson, B.A., Lovell, J.F., 2020. SARS-CoV-2 RBD Neutralizing antibody induction is enhanced by particulate vaccination. Adv. Mater. 32, 2005637 https://doi.org/10.1002/adma.202005637.

Hu, B., Zhao, X., Wang, E., Zhou, J., Li, J., Chen, J., Du, G., 2023. Efficient heterologous expression of cytochrome P450 enzymes in microorganisms for the biosynthesis of natural products. Crit. Rev. Biotechnol. 43, 227–241. https://doi.org/10.1080/07388551.2022.2029344.

Kandel, S.E., Lampe, J.N., 2014. Role of protein-protein interactions in cytochrome P450-mediated drug metabolism and toxicity. Chem. Res. Toxicol. 27, 1474–1486. https://doi.org/10.1021/tx500203s.

Kim, J.E., Jang, I.S., Son, S.H., Ko, Y.J., Cho, B.K., Kim, S.C., Lee, J.Y., 2019. Tailoring the *Saccharomyces cerevisiae* endoplasmic reticulum for functional assembly of terpene synthesis pathway. Metab. Eng. 56, 50–59. https://doi.org/10.1016/j.ymben.2019.08.013.

Kim, O.T., Um, Y., Jin, M.L., Kim, J.U., Hegebarth, D., Busta, L., Racovita, R.C., Jetter, R., 2018. A novel multifunctional C-23 Oxidase, CYP714E19, is involved in asiaticoside biosynthesis. Plant Cell Physiol. 59, 1200–1213. https://doi.org/10.1093/pcp/pcy055.

Lacaille-Dubois, M.A., 2019. Updated insights into the mechanism of action and clinical profile of the immunoadjuvant QS-21: a review. Phytomedicine 60, 152905. https://doi.org/10.1016/j.phymed.2019.152905.

Laurens, M.B., 2020. RTS,S/AS01 vaccine (Mosquirix™): an overview. Hum. Vaccin. Immunother. 16, 480–489. https://doi.org/10.1080/21645515.2019.1669415.

Li, W., Ma, X., Li, G., Zhang, A., Wang, D., Fan, F., Ma, X., Zhang, X., Dai, Z., Qian, Z., 2021. De novo biosynthesis of the oleanane-type triterpenoids of tunicosaponins in yeast. ACS Synth. Biol. 10, 1874–1881. https://doi.org/10.1021/acssynbio.1c00065.

Li, Y., Li, S., Thodey, K., Trenchard, I., Cravens, A., Smolke, C.D., 2018. Complete biosynthesis of noscapine and halogenated alkaloids in yeast. Proc. Natl. Acad. Sci. U. S. A. 115, E3922–E3931. https://doi.org/10.1073/pnas.1721469115.

Li, Z., Jiang, Y., Guengerich, F.P., Ma, L., Li, S., Zhang, W., 2020. Engineering cytochrome P450 enzyme systems for biomedical and biotechnological applications. J. Biol. Chem. 295, 833–849. https://doi.org/10.1074/jbc.REV119.008758.

Luo, X., Reiter, M.A., d'Espaux, L., Wong, J., Denby, C.M., Lechner, A., Zhang, Y., Grzybowski, A.T., Harth, S., Lin, W., Lee, H., Yu, C., Shin, J., Deng, K., Benites, V.T., Wang, G., Baidoo, E.E.K., Chen, Y., Dev, I., Petzold, C.J., et al., 2019. Complete biosynthesis of cannabinoids and their unnatural analogues in yeast. Nature 567, 123–126. https://doi.org/10.1038/s41586-019-0978-9.

Meesapyodsuk, D., Balsevich, J., Reed, D.W., Covello, P.S., 2007. Saponin biosynthesis in *Saponaria vaccaria*. cDNAs encoding beta-amyrin synthase and a triterpene carboxylic acid glucosyltransferase. Plant. Physiol. 143, 959–969. https://doi.org/10.1104/pp.106.088484.

Mayer, K., Schüller, C., Wambutt, R., Murphy, G., Volckaert, G., Pohl, T., Düsterhöft, A., Stiekema, W., Entian, K.D., Terryn, N., Harris, B., Ansorge, W., Brandt, P., Grivell, L., Rieger, M., Weichselgartner, M., de Simone, V., Obermaier, B., Mache, R., Müller, M., et al., 1999. Sequence and analysis of chromosome 4 of the plant *Arabidopsis thaliana*. Nature 402, 769–777. https://doi.org/10.1038/47134.

Moses, T., Pollier, J., Almagro, L., Buyst, D., Van Montagu, M., Pedreño, M.A., Martins, J. C., Thevelein, J.M., Goossens, A., 2014. Combinatorial biosynthesis of sapogenins and saponins in *Saccharomyces cerevisiae* using a C-16α hydroxylase from Bupleurum falcatum. Proc. Natl. Acad. Sci. U. S. A. 111, 1634–1639. https://doi.org/10.1073/pnas.1323369111.

Moses, T., Pollier, J., Faizal, A., Apers, S., Pieters, L., Thevelein, J.M., Geelen, D., Goossens, A., 2015. Unravelling the triterpenoid saponin biosynthesis of the African shrub *Maesa lanceolata*. Mol. Plant 8, 122–135. https://doi.org/10.1093/mp/ssu110.

Naseri, G., Koffas, M.A.G., 2020. Application of combinatorial optimization strategies in synthetic biology. Nat. Commun. 11, 2446. https://doi.org/10.1038/s41467-020-16175-y.

Nowrouzi, B., Rios-Solis, L., 2022. Redox metabolism for improving whole-cell P450-catalysed terpenoid biosynthesis. Crit. Rev. Biotechnol. 42, 1213–1237. https://doi.org/10.1080/07388551.2021.1990210.

Ozalp, C., Szczesna-Skorupa, E., Kemper, B., 2005. Bimolecular fluorescence complementation analysis of cytochrome p450 2c2, 2e1, and NADPH-cytochrome p450 reductase molecular interactions in living cells. Drug Metab. Dispos. 33, 1382–1390. https://doi.org/10.1124/dmd.105.005538.

Paddon, C.J., Westfall, P.J., Pitera, D.J., Benjamin, K., Fisher, K., McPhee, D., Leavell, M. D., Tai, A., Main, A., Eng, D., Polichuk, D.R., Teoh, K.H., Reed, D.W., Treynor, T., Lenihan, J., Fleck, M., Bajad, S., Dang, G., Dengrove, D., Diola, D., et al., 2013. High-level semi-synthetic production of the potent antimalarial artemisinin. Nature 496, 528–532. https://doi.org/10.1038/nature12051.

Papagiannidis, D., Bircham, P.W., Lüchtenborg, C., Pajonk, O., Ruffini, G., Brügger, B., Schuck, S., 2021. Ice2 promotes ER membrane biogenesis in yeast by inhibiting the conserved lipin phosphatase complex. EMBO J. 40, e107958 https://doi.org/10.15252/embj.2021107958.

Park, S.Y., Eun, H., Lee, M.H., Lee, S.Y., 2022. Metabolic engineering of *Escherichia coli* with electron channelling for the production of natural products. Nat. Catal. 5, 726–737. https://doi.org/10.1038/s41929-022-00820-4.

Partipilo, M., Ewins, E.J., Fralliccardi, J., Robinson, T., Poolman, B., Slotboom, D.J., 2021. Minimal pathway for the regeneration of redox cofactors. JACS. Au. 1, 2280–2293. https://doi.org/10.1021/jacsau.1c00406.

Peng, B., Wood, R.J., Nielsen, L.K., Vickers, C.E., 2018. An expanded heterologous GAL promoter collection for diauxie-inducible expression in *Saccharomyces cerevisiae*. ACS Synth. Biol. 7, 748–751. https://doi.org/10.1021/acssynbio.7b00355.

Podust, L.M., Sherman, D.H., 2012. Diversity of P450 enzymes in the biosynthesis of natural products. Nat. Prod. Rep. 29, 1251–1266. https://doi.org/10.1039/c2np20020a.

Reed, J., Orme, A., El-Demerdash, A., Owen, C., Martin, L.B.B., Misra, R.C., Kikuchi, S., Rejzek, M., Martin, A.C., Harkess, A., Leebens-Mack, J., Louveau, T., Stephenson, M. J., Osbourn, A., 2023. Elucidation of the pathway for biosynthesis of saponin adjuvants from the soapbark tree. Science 379, 1252–1264. https://doi.org/10.1126/science.adf3727.

Reichert, C.L., Salminen, H., Weiss, J., 2019. Quillaja saponin characteristics and functional properties. Annu. Rev. Food Sci. Technol. 10, 43–73. https://doi.org/10.1146/annurev-food-032818-122010.

Ryu, C.S., Klein, K., Zanger, U.M., 2017. Membrane associated progesterone receptors: promiscuous proteins with pleiotropic functions - focus on interactions with cytochromes p450. Front. Pharmacol. 8, 159. https://doi.org/10.3389/fphar.2017.00159.

Salanoubat, M., Lemcke, K., Rieger, M., Ansorge, W., Unseld, M., Fartmann, B., Valle, G., Blöcker, H., Perez-Alonso, M., Obermaier, B., Delseny, M., Boutry, M., Grivell, L.A., Mache, R., Puigdomènech, P., De Simone, V., Choisne, N., Artiguenave, F., Robert, C., Brottier, P., 2000. Sequence and analysis of chromosome 3 of the plant *Arabidopsis thaliana*. Kazusa DNA Research Institute Nature 408, 820–822. https://doi.org/10.1038/35048706.

Shah, R.A., Limmer, A.L., Nwannunu, C.E., Patel, R.R., Mui, U.N., Tyring, S.K., 2019. Shingrix for herpes zoster: a review. Skin. Therapy. Lett. 24, 5–7.

Shibuya, M., Katsube, Y., Otsuka, M., Zhang, H., Tansakul, P., Xiang, T., Ebizuka, Y., 2009. Identification of a product specific beta-amyrin synthase from *Arabidopsis thaliana*. Plant. Physiol. Biochem. 47, 26–30. https://doi.org/10.1016/j.plaphy.2008.09.007.

Sun, J., Sun, W., Zhang, G., Lv, B., Li, C., 2022. High efficient production of plant flavonoids by microbial cell factories: challenges and opportunities. Metab. Eng. 70, 143–154. https://doi.org/10.1016/j.ymben.2022.01.011.

Sun, W.T., Xue, H.J., Liu, H., Lv, B., Yu, Y., Wang, Y., Huang, M.L., Li, C., 2020. Controlling chemo- and regioselectivity of a plant P450 in yeast cell toward rare licorice triterpenoid biosynthesis. ACS Catal. 10, 4253–4260. https://doi.org/10.1021/acscatal.0c00128.

Urlacher, V.B., Girhard, M., 2019. Cytochrome P450 monooxygenases in biotechnology and synthetic biology. Trends Biotechnol. 37, 882–897. https://doi.org/10.1016/j.tibtech.2019.01.001.

Wallberg, A., Bunikis, I., Pettersson, O.V., Mosbech, M.B., Childers, A.K., Evans, J.D., Mikheyev, A.S., Robertson, H.M., Robinson, G.E., Webster, M.T., 2019. A hybrid de novo genome assembly of the honeybee, *Apis mellifera*, with chromosome-length scaffolds. BMC Genom. 20, 275. https://doi.org/10.1186/s12864-019-5642-0.

Walkowicz, W.E., Fernández-Tejada, A., George, C., Corzana, F., Jiménez-Barbero, J., Ragupathi, G., Tan, D.S., Gin, D.Y., 2016. Quillaja saponin variants with central glycosidic linkage modifications exhibit distinct conformations and adjuvant activities. Chem. Sci. 7, 2371–2380. https://doi.org/10.1039/C5SC02978C.

Wang, D., Wang, J., Shi, Y., Li, R., Fan, F., Huang, Y., Li, W., Chen, N., Huang, L., Dai, Z., Zhang, X., 2020. Elucidation of the complete biosynthetic pathway of the main triterpene glycosylation products of *Panax notoginseng* using a synthetic biology platform. Metab. Eng. 61, 131–140. https://doi.org/10.1016/j.ymben.2020.05.007.

Wang, P., Kim, Y.J., Navarro-Villalobos, M., Rohde, B.D., Gin, D.Y., 2005. Synthesis of the potent immunostimulatory adjuvant QS-21A. J. Am. Chem. Soc. 127, 3256–3257. https://doi.org/10.1021/ja0422007.

Yang, C., Li, W., Li, C., Zhou, Z., Xiao, Y., Yan, X., 2018. Metabolism of ganoderic acids by a *Ganoderma lucidum* cytochrome P450 and the 3-keto sterol reductase ERG27 from yeast. Phytochemistry 155, 83–92. https://doi.org/10.1016/j.phytochem.2018.07.009.

Yang, J., Liang, J., Shao, L., Liu, L., Gao, K., Zhang, J.L., Sun, Z., Xu, W., Lin, P., Yu, R., Zi, J., 2020. Green production of silybin and isosilybin by merging metabolic engineering approaches and enzymatic catalysis. Metab. Eng. 59, 44–52. https://doi.org/10.1016/j.ymben.2020.01.007.

Zhang, G., Cao, Q., Liu, J., Liu, B., Li, J., Li, C., 2015. Refactoring β-amyrin synthesis in *Saccharomyces cerevisiae*. AIChE J. 61, 3172–3179. https://doi.org/10.1002/aic.14950.

Zhang, J., Hansen, L.G., Gudich, O., Viehrig, K., Lassen, L.M.M., Schrübbers, L., Adhikari, K.B., Rubaszka, P., Carrasquer-Alvarez, E., Chen, L., D'Ambrosio, V., Lehka, B., Haidar, A.K., Nallapareddy, S., Giannakou, K., Laloux, M., Arsovska, D., Jørgensen, M.A.K., Chan, L.J.G., Kristensen, M., et al., 2022. A microbial supply chain for production of the anti-cancer drug vinblastine. Nature 609, 341–347. https://doi.org/10.1038/s41586-022-05157-3.

Zhao, Y.J., Li, C., 2018. Biosynthesis of plant triterpenoid saponins in microbial cell factories. J. Agric. Food Chem. 66, 12155–12165. https://doi.org/10.1021/acs.jafc.8b04657.

Zhu, Y., Xu, J., Sun, C., Zhou, S., Xu, H., Nelson, D.R., Qian, J., Song, J., Luo, H., Xiang, L., Li, Y., Xu, Z., Ji, A., Wang, L., Lu, S., Hayward, A., Sun, W., Li, X., Schwartz, D.C., Wang, Y., et al., 2015. Chromosome-level genome map provides insights into diverse defense mechanisms in the medicinal fungus *Ganoderma sinense*. Sci. Rep. 5, 11087 https://doi.org/10.1038/srep11087.